IEEE Photonics Journal
An IEEE Photonics Society Publication

Nonsequential Speckle Reduction Method by Generating Uncorrelated Laser Subbeams With Equivalent Intensity Using a Reflective Spatial Light Modulator

Volume 9, Number 5, October 2017

Zhaomin Tong
Shaohua Song
Suotang Jia
Xuyuan Chen

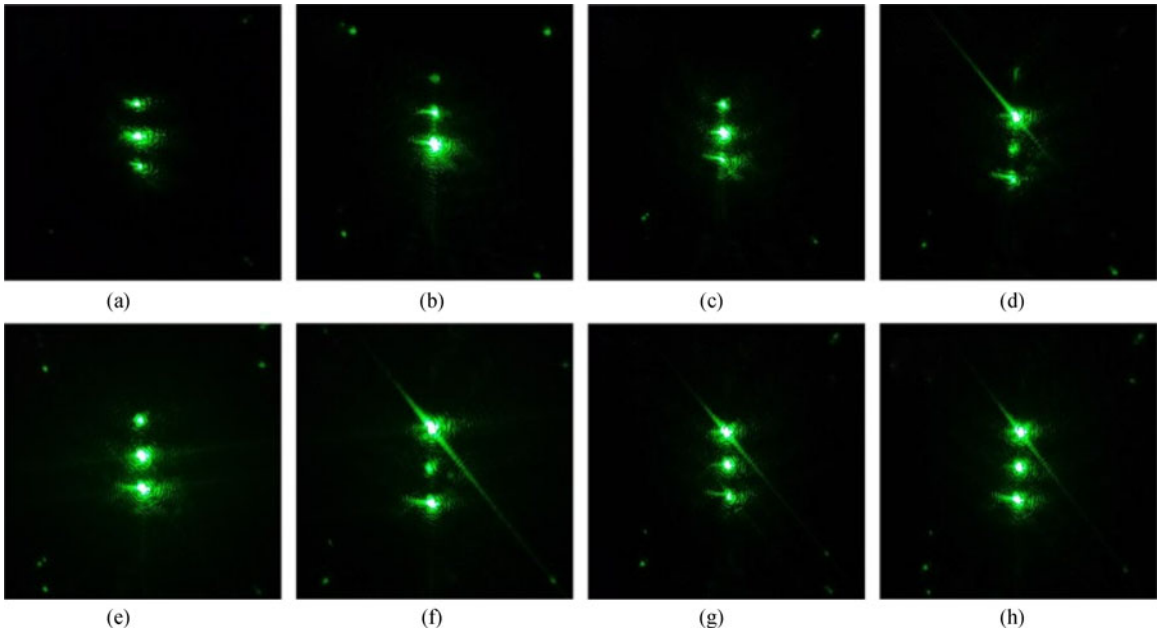

DOI: 10.1109/JPHOT.2017.2732507
1943-0655 © 2017 IEEE

Nonsequential Speckle Reduction Method by Generating Uncorrelated Laser Subbeams With Equivalent Intensity Using a Reflective Spatial Light Modulator

Zhaomin Tong,[1,2] Shaohua Song,[1,2] Suotang Jia,[1,2] and Xuyuan Chen[1,2,3]

[1]State Key Laboratory of Quantum Optics and Quantum Optics Devices, Institute of Laser Spectroscopy, Shanxi University, Taiyuan 030006, China
[2]Collaborative Innovation Center of Extreme Optics, Shanxi University, Taiyuan 030006, China
[3]Faculty of Technology and Maritime Sciences, Department of Micro- and Nanosystem Technology, University College of Southeast Norway, Borre N-3184, Norway

DOI:10.1109/JPHOT.2017.2732507

Manuscript received June 20, 2017; revised July 20, 2017; accepted July 24, 2017. Date of publication July 27, 2017; date of current version August 17, 2017. This work was supported in part by the National Key Research and Development Program of China under Grant 2016YFB0401903 and Grant 2016YFB0402003, in part by the National Natural Science Foundation of China (NSFC) under Grant 61404104, in part by the Key Research and Development Program of Shanxi Province for International Cooperation under Grant 201703D421015, in part by the Natural Science Foundation of Jiangsu Province under Grant BK20140409, in part by the Changjiang Scholars and Innovative Research Team in University of Ministry of Education of China under Grant IRT13076, and in part by the State Key Program of National Natural Science of China under Grant 11434007. Corresponding author: Zhaomin Tong (e-mail: zhaomin.tong@sxu.edu.cn).

Abstract: Sequential speckle reduction methods demand the usage of fast modulators due to the short integration period of human eyes. Here, a nonsequential speckle reduction method by splitting one laser beam with short coherence length into uncorrelated laser subbeams (LSBs) is reported. In order to realize the most efficient speckle reduction, with the help of a polarization beam splitter, we have programmed a reflective spatial light modulator to make the LSBs intensities equivalent. Three uncorrelated LSBs with equivalent light intensity are designed to demonstrate this idea; the speckle contrast ratio is reduced to 0.55, which closes to the expected value of 0.58. This nonsequential speckle reduction method has no requirement of the modulators speed; thus, it has obvious merit comparing with the sequential speckle reduction methods.

Index Terms: Coherent effects, coherent imaging.

1. Introduction

With the fast development of high-power and low-cost semiconductor lasers, laser display industry grows rapidly in the past decade [1]–[3]. Speckle, however, is a problem in laser displays and is needed to be suppressed. Currently, sequential speckle reduction methods by vibrating screen or by changing diffuser etc. are the most commonly used technologies [4]–[8]. The speckle reduction mechanism of these methods is the formation of different speckle patterns and the summation of them during one human eye integration period (∼50 ms) [9]. In order to bring the speckle contrast ratio (CR) on the screen down to the critical value that human eyes cannot detect (lowest level

at 3.2% for green color) [10], and if the screen depolarization (introducing extra two degrees of speckle reduction freedom) is the only other independent speckle reduction mechanism that is compounded, the number of the summed independent speckle patterns should be larger than $(1/0.032)^2/2 \approx 488$ [11]. Therefore, the realization period for each independent speckle patterns must be shorter than $50/488 \approx 0.1$ ms. Mechanical vibrators or rotators are generally used as the fast modulators, which are bulky and may have the reliability problem (for example, the screen deforms permanently). In our previous publications, we have reported the development of more compact sequential speckle reduction methods by modulating laser beams either with a micro-scanning mirror or with a diffractive optical element [12]–[15], and by programming a binary micromirror array or a ferroelectric spatial light modulator (SLM) [16], [17]. However, these techniques also require using modulators working at high speed.

Currently, laser diodes (LDs) are the preferred cost-effective illumination light sources in laser displays [2]. The coherence length of LDs is short (on the order of centimeters) [16]; thus, we can easily destroy the temporal coherence of LDs and reduce speckle by introducing proper light delays [11]. Based on this analysis, in this paper, we propose a non-sequential speckle reduction method by using a reflective SLM and a polarization beam splitter (PBS), where one laser beam is split as several uncorrelated laser sub-beams with equivalent intensity. With the proposed method, the requirement of using fast modulators in sequential speckle reduction methods can be avoided. This is especially superior when the well-developed nematic liquid crystal (LC) material is used. The typical response time of the nematic LC material is on the order of milliseconds [18]. In order to efficiently reduce speckle in laser displays by using the sequential speckle reduction methods, the nematic LC material is obviously too slow to generate sufficient large numbers of independent speckle patterns during the integration period of human eyes.

2. Theory and Experiment

The speckle CR C is defined as the ratio between the standard deviation σ_I and the mean value $\overline{I}$ of the light intensity, such as [11]

$$C = \frac{\sigma_I}{\overline{I}}. \tag{1}$$

If N speckle patterns are summed together to form an averaged speckle pattern, where the mth and nth speckle pattern intensities are $\overline{I_m}$ and $\overline{I_n}$ and their correlation coefficient is $\rho_{m,n}$, the speckle CR of the summed speckle pattern C_s can be written as

$$\begin{aligned} C_s &= \frac{\sqrt{\overline{\left(\sum_{n=1}^{N} I_n\right)^2} - \overline{\sum_{n=1}^{N} I_n}^2}}{\overline{\sum_{n=1}^{N} I_n}} \\ &= \frac{\sqrt{\sum_{m=1}^{N}\sum_{n=1}^{N} \overline{I_m I_n} - \left(\sum_{n=1}^{N} \overline{I_n}\right)^2}}{\sum_{n=1}^{N} \overline{I_n}} \\ &= \frac{\sqrt{\sum_{m=1}^{N}\sum_{n=1}^{N} \left[\overline{I_m I_n} + \rho_{m,n}\sqrt{\overline{(I_m - \overline{I_m})^2 (I_n - \overline{I_n})^2}}\right] - \left(\sum_{n=1}^{N} \overline{I_n}\right)^2}}{\sum_{n=1}^{N} \overline{I_n}}. \end{aligned} \tag{2}$$

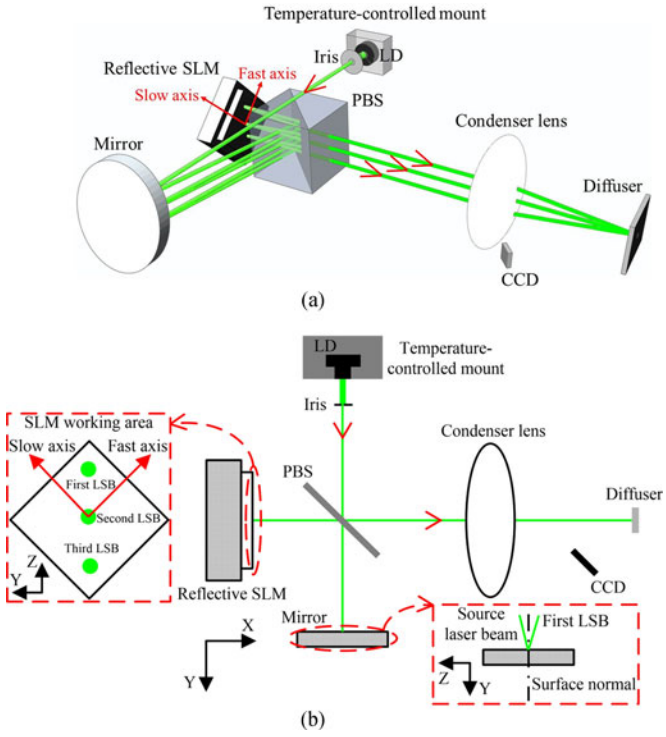

Fig. 1. Schematic diagrams of the proposed non-sequential speckle reduction method with (a) a 3D drawing and (b) a 2D drawing, where three uncorrelated LSBs with equivalent intensity are designed to use. (SLM, spatial light modulator; PBS, polarization beam splitter). The source laser beam from the LD illuminates the mirror at a non-zero angle of incidence, which results in the multiple reflections on the different areas of the reflective SLM.

According to (2), the speckle CR C_s is proportional to the value of the correlation coefficient $\rho_{m,n}$; thus, when $\rho_{m,n} = 0$, contribution of the summed speckle pattern correlations on the speckle CR C_s can be ignored, and the speckle CR C_s can be reduced to

$$C_s = \frac{\sqrt{\sum_{m=1}^{N}\sum_{n=1}^{N}\overline{I_m I_n} - \left(\sum_{n=1}^{N}\overline{I_n}\right)^2}}{\sum_{n=1}^{N}\overline{I_n}} = \frac{\sqrt{\sum_{n=1}^{N}\overline{I_n}^2}}{\sum_{n=1}^{N}\overline{I_n}}. \tag{3}$$

The speckle CR C_s can be further reduced to the minimum value at $C_{s\_\min} = 1/N^{1/2}$ when the light intensities for each speckle pattern are equal, such as $\overline{I_m} = \overline{I_n}$.

Based on the above theoretical analysis, in order to reduce speckle most efficiently, two design guidelines must be followed in our experiments: firstly, we should make the speckle patterns uncorrelated; and secondly, we must make the light intensities of the speckle patterns equivalent. Fig. 1 schematically shows the experimental setup. A collimated s-polarized 50 mW green LD (L520P50 from Thorlabs) is used as the light source. Operating temperature of the LD is maintained at 10 °C by a temperature-controlled mount (LTC100-A from Thorlabs), where the central wavelength and the full width at half maximum of the LD are measured by a spectrometer (ARYELLE Butterfly from LTB) as $\lambda = 513.8$ nm and $\triangle\lambda = 0.69$ nm, respectively. A 0.5 mm in diameter circular iris is placed after the LD to determine the effective laser beam width. The s-polarized source laser beam directly illuminates a metallic coated mirror (PF10-03-G01 from Thorlabs) at a non-zero angle of incidence, and it is reflected by the PBS (PBS251 from Thorlabs, ~5% transmission for the s-polarized light) to the reflective SLM (HSPDM512 from Meadowlark). The pixel size of the SLM is 15 μm × 15 μm. The fill factor of the SLM is 100%, which provides high zero-order diffraction efficiency at 90–95%

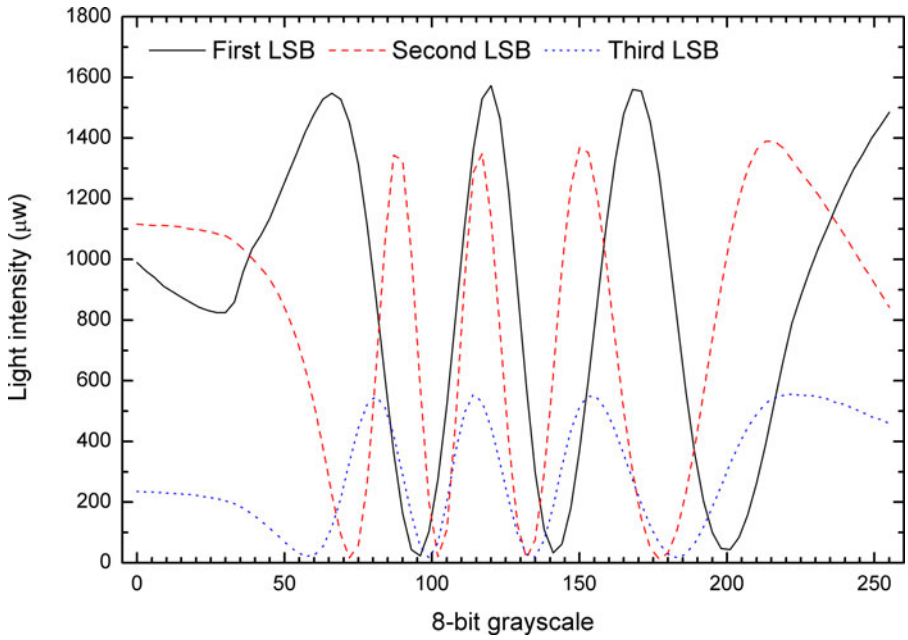

Fig. 2. Relationships between the 8-bit grayscales of the reflection area on the reflective SLM and the light intensities of the LSBs. The relationship for the first LSB (black solid line) was characterized at first, and then the relationship for the second LSB (red dash line) was measured when the grayscale of the first reflection area on the reflective SLM equaling to $GS_{v1} = 141$. Finally, the relationship for the third LSB (blue dot line) was obtained, where the grayscales of the first and second reflection areas on the reflective SLM were set at $GS_{v1} = 141$ and $GS_{v2} = 135$, respectively.

[19]. Slow axis of the reflective SLM is fixed as 45° along the vertical direction, and the pixels grayscales of the reflective SLM coving the first reflection area are programmed at a same value. The PBS splits the first reflected elliptically polarized light from the reflective SLM as s- and p-polarized laser sub-beams (LSBs), where the reflected s-polarized LSB illuminates the mirror and contributes to further reflections, and the transmitted p-polarized LSB (PBS transmits ∼95% p-polarized light) forms speckle on a silver-coated reflecting diffuser. Due to the limited array size of the reflective SLM (7.68 mm × 7.68 mm), the number of reflections on the reflective SLM is limited as three. For the second and third reflections, similar optical paths are guided by the mirror, the PBS and the reflective SLM. However, different reflection areas on the reflective SLM are used, and we programmed the pixels grayscales of the second and third reflection areas at other individual values, respectively. Finally, with the help of an $f = 50$ mm condenser lens, we can obtain three p-polarized LSBs which illuminate the diffuser along different directions. A charge-coupled device (CCD) camera is placed before the diffuser to record the speckle patterns.

As shown in Fig. 1, the distances between the mirror and the PBS and between the PBS and the reflective SLM are 40 mm and 5 mm, respectively. The refractive index of the 25.4 mm cubic PBS equals to ∼1.7. By assuming that the angle of incidence of the source laser beam on the mirror equals to zero, we can calculate that the $(n+1)$th LSB is delayed by ∼ 176 mm to the nth LSB, where $n = 1$ or $n = 2$. The coherence length of the LD approximately equals to $\lambda^2/\triangle\lambda = 383\ \mu$m [18], which is much shorter than the light delays among the LSBs; thus, the three LSBs are uncorrelated.

The procedure to make the LSBs intensities equivalent is as follows: firstly, we characterized the light intensity of the first LSB by changing the 8-bit grayscales of the first reflection area on the reflective SLM from 0 to 255. By placing an integrating sphere optical power meter (S142C from Thorlabs) between the PBS and the condenser lens in Fig. 1, we measured the light intensity of each LSB. The relationship between the 8-bit grayscale of the first reflection area on the reflective SLM and the light intensity of the first LSB is plotted in Fig. 2 (black solid line), where the peak intensity of $I_{p1} = 1573\ \mu$W at grayscale of $GS_{p1} = 120$ and the valley intensity

of $I_{v1} = 33\,\mu$W at grayscale of $GS_{v1} = 141$ are found; secondly, we measured the relationship between the 8-bit grayscale of the second reflection area on the reflective SLM and the light intensity of the second LSB when $GS_{v1} = 141$, which is also plotted in Fig. 2 (red dash line). We can find the peak and valley intensities $I_{p2} = 1350\,\mu$W and $I_{v2} = 15\,\mu$W at grayscales of $GS_{p2} = 117$ and $GS_{v2} = 135$, respectively; thirdly, by setting $GS_{v1} = 141$ and $GS_{v2} = 135$, we measured the relationship between the 8-bit grayscale of the third reflection area on the reflective SLM and the light intensity of the third LSB. The results are shown in Fig. 2 too (blue dot line), where the peak intensity $I_{p3} = 555\,\mu$W at the grayscale of $GS_{p3} = 114$ and the valley intensity $I_{v3} = 19\,\mu$W at the grayscale of $GS_{v3} = 135$ are found. Assume that the optical power loss caused by the PBS is negligible, there are two other optical power loss mechanisms in these measurements: partial reflection (~90% for each reflection) of the mirror and the imperfect zero-order diffraction efficiency of the reflective SLM (90%–95%). The PBS has a transmitted beam extinction ratio equaling to 1000:1, thus, it is acceptable to simplify the calculations of the optical power losses in percentage by using the following relationships:

$$\eta_{Loss1} = \frac{I_{P1} - I_{p2}}{I_{P1}} \times 100\%,$$
$$\eta_{Loss2} = \frac{I_{P2} - I_{p3}}{I_{P2}} \times 100\%, \tag{4}$$

where we have assumed that the PBS perfectly reflects the s-polarized light and transmits the p-polarized light, and η_{Loss1} and η_{Loss2} represent the optical power losses in percentage between the second LSB and the first LSB and between the third LSB and the second LSB, respectively. By substituting the values of the measured peak intensities I_{p1}, I_{p2} and I_{p3}, we found $\eta_{Loss1} = 14.2\%$ and $\eta_{Loss2} = 58.9\%$. Next, by assuming the equivalent intensity of the LSBs is a value of I_e, we have

$$3I_e = I_{p1} - I_{loss1} - I_{loss2}, \tag{5}$$

where I_{loss1} and I_{loss2} represent the optical power losses between the second LSB and the first LSB and between the third LSB and the second LSB, respectively. The expressions to calculate I_{loss1} and I_{loss2} can be written as

$$I_{loss1} = (I_{p1} - I_e) \times \eta_{loss1},$$
$$I_{loss2} = (I_{p1} - 2I_e - I_{loss1}) \times \eta_{loss2}. \tag{6}$$

After solving Eqs. (4)-(6), we found $I_e \approx 315.7\,\mu$W. Therefore, the reflection areas grayscales on the reflective SLM should be set at the values where the intensities of the LSBs shown in Fig. 2 equal to $I_e = 315.7\,\mu$W for the first LSB, $I_e \times I_{p2}/(I_{p1} - I_e - I_{loss1}) = 395.1\,\mu$W for the second LSB, and $I_{p3} = 555\,\mu$W for the third LSB, respectively. According to Fig. 2, these grayscales were found as $GS_{e1} = 134$, $GS_{e2} = 126$ and $GS_{e3} = 114$ for the first, second and third reflection areas on the reflective SLM, respectively.

Similar procedures could be employed to determine the grayscales when we designed two LSBs with equivalent intensity, such as $GS_{e1} = 130$, $GS_{e2} = 117$ and GS_{e3} equaling to an arbitrary value when the first and second LSBs were used, $GS_{e1} = 134$, $GS_{e2} = 135$ and $GS_{e3} = 114$ when the first and third LSBs were used, and $GS_{e1} = 141$, $GS_{e2} = 126$ and $GS_{e3} = 114$ when the second and third LSBs were used, respectively. After placing a reflective screen in between the PBS and the condenser lens in Fig. 1, laser spots from the LSBs were recorded by a camera focusing on the reflective screen.

3. Results and Discussions

Fig. 3 shows the captured laser spots by modulating the LSBs intensities when the reflective SLM was switched off, and when one LSB, and two LSBs or three LSBs with equivalent intensity were designed to use, respectively.

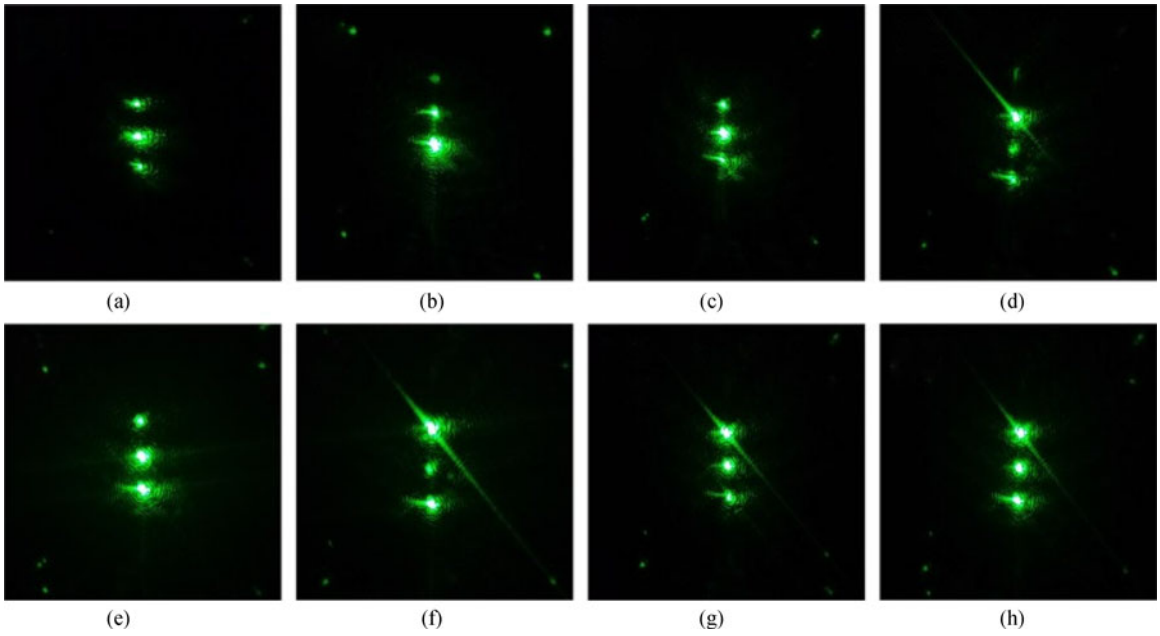

Fig. 3. Laser spots when the LSBs intensities were modulated. (a) The reflective SLM was switched off; (b)–(d) only the first LSB (the bottom laser spot), the second LSB (the middle laser spot) or the third LSB (the top laser spot) was designed to use, respectively; (e)–(g) the first and second LSBs with equivalent intensity, the first and third LSBs with equivalent intensity, or the second and third LSBs with equivalent intensity were designed to use, respectively; and (h) when the three LSBs with equivalent intensity were designed to use.

As we can find in Figs. 2 and 3, because the transmitted beam extinction ratio of the PBS is not very high, we cannot make the light intensities of LSBs that are not intended to generate as zero. Ratios among light intensities of the first LSB (the bottom laser spot in Fig. 3), the second LSB (the middle laser spot in Fig. 3) and the third LSB (the up laser spot in Fig. 3) were measured and listed as follows: 1:0.2:0.08 in Fig. 3(b), 0.5:1:0.31 in Fig. 3(c), 0.18:0.13:1 in Fig. 3(d), 1:0.93:0.32 in Fig. 3(e), 0.59:0.22:1 in Fig. 3(f), 0.44:0.72:1 in Fig. 3(g), and 0.85:0.81:1 in Fig. 3(h). According to these measured values, light intensities of the intended to be used LSBs are not exactly equivalent. This is reasonable because in our designed procedure, we assume that the PBS perfectly reflects the s-polarized light and transmits the p-polarized light; thus, the expressions for the optical power losses in percentage given in (2) are not completely correct.

By substituting the measured ratios among light intensities of the first LSB, the second LSB and the third LSB into (3), the speckle CRs for the conditions presented in Figs. 3(b)–(h) were calculated, such as 0.8, 0.69, 0.78, 0.62, 0.65, 0.61 and 0.58, respectively. Fig. 4 shows the speckle patterns captured by the CCD camera and the speckle CRs corresponding to the conditions shown in Fig. 3. We can find that the speckle reduction trend in the experiments is consistent with our predictions; however, differences between the experimental results and the expected values are observed. Possible cause of this difference is that the high-order diffracted laser beams by the reflective SLM were used to form the speckle patterns in Fig. 4; thus, ratios among light intensities of the LSBs are not exact, and error were introduced when we calculated the speckle CRs.

Due to the limited array size of the reflective SLM, we can only equalize maximum three LSBs intensity and demonstrate the feasibility of this non-sequential speckle reduction method. However, with specifically designed liquid crystal phase retarders, we expect to generate more LSBs in one- or two-dimension with equivalent intensities to reduce speckle more efficiently. Based on (3), if the number of the generated uncorrelated LSBs with equivalent intensities equals to N (*i.e.*, the generated number of independent speckle patterns with equivalent intensities equals to N), the speckle CR can be reduced to $1/(2N)^{1/2}$ after compounding the two degrees of speckle reduction

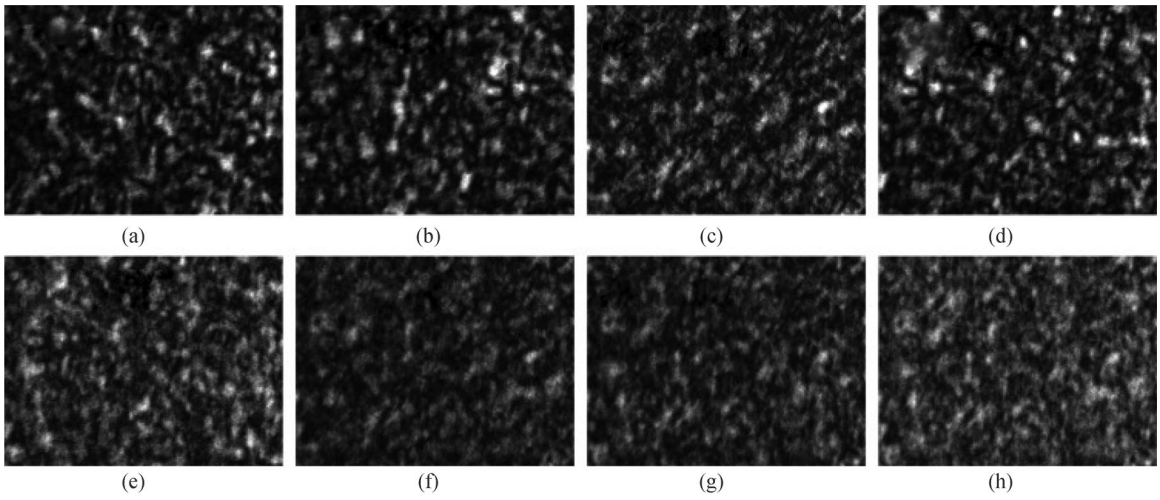

Fig. 4. Speckle patterns with the calculated speckle CRs. The results were obtained when the LSBs presented in Fig. 3 were used, where (a) the first row first column picture corresponds to Fig. 3(a), (b) the first row second column picture corresponds to Fig. 3(b), etc. (a) C = 0.89. (b) C = 0.91. (c) C = 0.78. (d) C = 0.91. (e) C = 0.65. (f) C = 0.64. (g) C = 0.62. (h) C = 0.55.

freedom caused by the screen depolarization. For example, we may generate 488 LSBs with equivalent intensities to reduce the speckle CR to 3.2% in Fig. 1 [11]. Depending on the laser beam width, each redesigned liquid crystal phase retarder can work as a polarization modulator with only one large pixel; thus, no high-order diffracted laser beams exist, and the optical power loss of the system can be reduced, so that we can predesign the equivalence among LSBs intensities more exactly. Furthermore, we can find that when the gray levels for each LSB are optimized for equivalent intensity, there is no need to vary the applied voltage for each pixel to change the LC orientations in our experiments; thus, the applied voltages of the specifically designed liquid crystal phase retarders can be fixed values.

The disadvantages of the proposed non-sequential speckle reduction method are that the optical system will be more complex and bulky than the sequential speckle reduction methods. This is because besides the LC modulator, the PBS must be introduced in this method, and more LSBs shall be generated to realize a more efficient speckle reduction. In theory, any compounded independent speckle reduction methods can result in further speckle reductions [11]. Therefore, the combination of non-sequential and sequential speckle reduction approaches can contribute to a lower speckle CR.

4. Conclusions

In summary, we proposed a non-sequential speckle reduction method. In order to make the LSBs intensity equivalent for most efficient speckle reduction, we introduced a reflective SLM and presented the design procedure. The proposed method has been verified experimentally, where speckle was successfully reduced. Inspired by this observation, it is expected to avoid the critical requirement of the modulators operating speed in sequential speckle reduction techniques; thus, the usage of slow modulators, for example, the modulators fabricated by using the well-developed nematic LC material, for speckle reduction in laser displays becomes possible.

In the future, we intend to design and fabricate special liquid crystal phase retarders with large pixel size, where each liquid crystal phase retarder can modulate the intensity of an individual LSB; thus, the diffraction effect of using many SLM pixels can be fully eliminated. Meanwhile, more LSBs with equivalent intensity can be generated depending on the number of the used special liquid crystal phase retarders.

References

[1] L. Jiang *et al.*, "GaN-based green laser diodes," *J. Semicond.*, vol. 37, no. 11, 2016, Art. no. 111001.
[2] K. V. Chellappan, E. Erden, and H. Urey, "Laser-based displays: a review," *Appl. Opt.*, vol. 49, no. 25, pp. F79–F98, 2010.
[3] G. Verschaffelt *et al.*, "Speckle disturbance limit in laser-based cinema projection systems," *Sci. Rep.*, vol. 5, 2015, Art. no. 14105.
[4] J. I. Trisnadi, "Hadamard speckle contrast reduction," *Opt. Lett.*, vol. 29, no. 1, pp. 11–13, 2004.
[5] S. C. Shin *et al.*, "Removal of hot spot speckle on laser projection screen using both the running screen and the rotating diffuser," *J. Display Technol.*, vol. 27, no. 3, pp. 91–96, 2006.
[6] S. Kubota and J. W. Goodman, "Very efficient speckle contrast reduction by moving diffuser device," *Appl. Opt.*, vol. 49, no. 23, pp. 4385–4391, 2010.
[7] J. Lee, T. Kim, B. Yim, J. Bu, and Y. Kim, "Speckle reduction in laser picoprojector by combining optical phase matrix with twin green lasers and oscillating MEMS mirror for coherence suppression," *Jpn. J. Appl. Phys.*, vol. 55, 2016, Art. no. 08RF03.
[8] J. Pan and C. Shih, "Speckle noise reduction in the laser mini-projector by vibrating diffuser," *J. Opt.*, vol. 19, 2017, Art. no. 045606.
[9] S. Roelandt, Y. Meuret, G. Craggs, G. Verschaffelt, P. Janssens, and H. Thienpont, "Standardized speckle measurement method matched to human speckle perception in laser projection systems," *Opt. Exp*, vol. 20, no. 8, pp. 8770–8783, 2012.
[10] G. Verschaffelt *et al.*, "Speckle disturbance limit in laser based cinema projection systems," *Sci. Rep.*, no. 5, 2015, Art. no. 14105.
[11] J. W. Goodman, *Speckle Phenomena in Optics: Theory and Applications*. Englewood, CO, USA: Roberts and Company Publishers, 2006.
[12] M. N. Akram, V. Kartashov, and Z. Tong, "Speckle reduction in line-scan laser projectors using binary phase codes," *Opt. Lett.*, vol. 35, no. 3, pp. 444–446, 2010.
[13] Z. Tong, X. Chen, M. N. Akram, and A. Aksnes, "Compound speckle characterization method and reduction by optical design," *J. Display Technol.*, vol. 8, no. 3, pp. 132–137, 2012.
[14] Z. Tong *et al.*, "Combination of micro-scanning mirrors and multi-mode fibers for speckle reduction in high lumen laser projector applications," *Opt. Exp*, vol. 25, no. 4, pp. 3795–3804, 2017.
[15] G. Ouyang *et al.*, "Speckle reduction using a motionless diffractive optical element," *Opt. Lett.*, vol. 35, no. 17, pp. 2852–2854, 2010.
[16] Z. Tong and X. Chen, "Principle, design and fabrication of a passive binary micro-mirror array (BMMA) for speckle reduction in grating light valve (GLV) based laser projection display," *Sensor. Actuat. A-Phys.*, vol. 210, pp. 209–216, 2014.
[17] Z. Tong and X. Chen, "A ferroelectric liquid crystal spatial light modulator encoded with orthogonal arrays and its optimized design for laser speckle reduction," *Opt. Laser Eng.*, vol. 90, pp. 173–178, 2017.
[18] B. E. A. Saleh and M. C. Teich, *Fundamentals of Photonics*. Hoboken, NJ, USA: Wiley, 2009.
[19] 2017. [Online]. Available: http://www.meadowlark.com/images/files/SLM—XY-Series-Sml-512x512-Specs.gif